LASER SHOCK COMPRESSION OF COPPER MONOCRYSTALS: MECHANISMS FOR DISLOCATION AND VOID GENERATION

M. A. MEYERS, M. S. SCHNEIDER, B. K KAD, V. A. LUBARDA,
University of California, San Diego, La Jolla, California 92093, USA

F. GREGORI
University of Paris 13, France

D.H. KALANTAR, B.A. REMINGTON,
Lawrence Livermore National Laboratory, Livermore, California 94450, USA

M. A. MEYERS, M. S. SCHNEIDER, B. K KAD, V. A. LUBARDA, F. GREGORI,
D.H. KALANTAR, B.A. REMINGTON,

Abstract. Copper with two orientations ([001] and [134]) was subjected to high intensity laser (energy levels of 40-300 J; energy densities of 15-70 MJ/m^2 and durations below 10 ns). The defects created are characterized by transmission electron microscopy. An orientation-dependent threshold stress for twinning is observed. The results are rationalized in terms of a criterion in which slip and twinning are considered as competing mechanisms. A constitutive description is applied to the two orientations, incorporating both slip and twinning. The predictions are in agreement with experiments. The threshold stress for twinning in the [001] orientation is 20-40 GPa, whereas the one for the [134] orientation is 40-60 GPa. The threshold stress is calculated, considering the effect of shock heating. The constitutive description provides a rationale for the experimental results; the calculated thresholds are 18 GPa for [001] and 25 GPa for [134]. A mechanism for void generation and growth based on the emission of geometrically necessary dislocations is proposed and analytically formulated.

1. INTRODUCTION

The effects of shock waves on metals have been studied for over fifty years [1]. Most experiments have used explosives and flyer plates as the means of creating the compression pulse. The short duration of the shock pulse ($0.1 - 2$ μs) renders direct measurements very difficult, if not impossible, and the mechanisms of plastic deformation have to be inferred from post-shock examination of the residual defect substructure. It is only recently [2,3] that pulsed x-ray diffraction has been used to obtain quantitative information of the lattice distortions at the shock front. Recent experiments by Meyers et al. [4] using copper single crystal specimens showed that dislocation configurations and twinning threshold using laser-induced shock waves are very similar to those obtained at durations 10 – 100 times longer as in explosively driven flyer plate studies. The early experiments by Johari and Thomas [5] and more recent results by Murr [6], Grace [7] and Gray [8] showed cell sizes which decreased with increasing shock pressures. These results are a clear confirmation that defects are generated at the shock front, corroborating the theoretical treatment of Smith [1], Hornbogen [9], Meyers [10], Weertman [11] and Mogilevskii [12].

2. EXPERIMENTAL TECHNIQUES

The shock experiments were carried out at the OMEGA Laser Facility at University of Rochester's Laboratory for Laser Energetics (LLE) and at the LLNL Janus facility. The input laser energies used in the experiments are for [001]: 40 J, 70 J, 205 J, and 300 J; and for [$\bar{1}$34]: 70 J, 205 J and 300 J. The laser spot size was on the order of 2.5 mm to 3.0 mm depending on the size of the sample and the pulse duration is typically 2.5 ns with a small number of experiments occurring at 10 ns. The energies can be translated into pressures using Lindl's equation [13]

$$P = 40\left(\frac{I_{15}}{\lambda}\right)^{2/3} \quad , \tag{1}$$

where P is pressure (Mbar), I_{15} is laser intensity (10^{15} w/cm^2), and λ is wavelength in micrometers. Thus, 40 J is equivalent to an initial pressure of 12 GPa, 70 J equivalent to 20 GPa, 205 J equivalent to 40 GPa, and 300 J equivalent to 60 GPa. The results of six shock recovery conditions are reported herein. Thin foils were prepared from samples cut at standard distances from the energy deposition surface. This enabled the direct observation of the change in residual microstructure with pulse decay that can be predicted from computational simulations as shown in Figure 1.
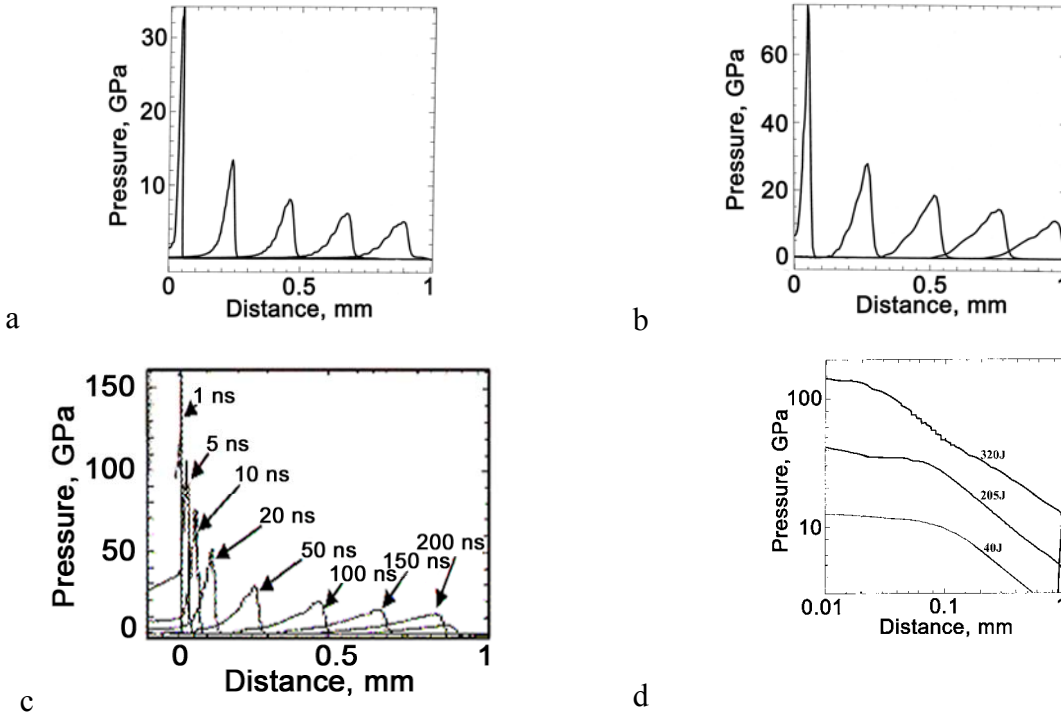

Figure 1. Simulated pressure profiles as a function of distance from energy deposition surface for three different laser impact energies: (a) 70 J; (b) 200 J; and (c) 300 J. (d) Maximum pressure as function of distance from impacted surface for the three shock impact energies shown in (a)-(c). For each condition, the shock wave exponentially decreases in amplitude with distance traveled.

3. RESULTS OF TRANSMISSION ELECTRON MICROSCOPY

The [001] orientation shocked at 20 GPa contains a well-defined cellular organization of 1/2<110> dislocations with average dimensions between 0.2 and 0.3 μm cell size, Figure 2(a). The microstructure was homogeneous throughout the sample. Qualitatively, these results confirm previous observations, albeit at a pulse duration that is lower by a factor of 10-100 than that applied by Murr [6]. The predicted cell size from Murr's plot [6] at a pressure of 12 GPa is 0.4 μm. The observed cell size is also consistent with Gray's [8] measurements: 0.5 μm/10 GPa. The [$\bar{1}34$] orientation shocked at 20 GPa contains a similar well-defined cellular network comprised of 1/2<110> dislocations with a slightly larger (0.3-0.4 μm) average cell size, Figure 2(c). The dislocation density is on the order of 10^{13} m^{-2}.

For 40 GPa, the [001] orientation, this intermediate energy input creates dense dislocation tangles, stacking faults, and micro-twins, Figure 2(b). There are no readily discernible dislocation cells. Furthermore, the observed deformation sub-structure appears uniform around the thin foil perforation. These features are significantly different than the deformation substructure observed at the lower impact energy, Figure 2(a), in what can be construed as a pressure-dependent change in the deformation mechanism. Perpendicular traces of planar features are seen when the beam direction is <001>. These correspond to traces of {111} on (001). All four stacking fault variants *viz* the

$(11\bar{1})1/6[112]$, $(111)1/6[\bar{1}\,\bar{1}\,2]$, $(\bar{1}11)1/6[1\,\bar{1}\,2]$, and $(1\bar{1}1)1/6[\bar{1}\,1\,2]$ are observed. Given the incident energy input as parallel to [001], it is not surprising that all four stacking fault variants are activated, Figure 2(b), as they all have the same Schmid factor. For the $[\bar{1}34]$ orientation, the deformation substructure continues to be cellular, albeit finer at a 0.15 μm average cell size and a significantly higher dislocation density, 10^{14} m^{-2}, Figure 2(d). This is in direct contrast to the mechanism change observed in [001]. Again, the three slip systems previously described dominate the deformation substructure. A large number of loops were also visible. These were found to contribute to the cell walls and were often commonly found within the cells in a very low concentration.
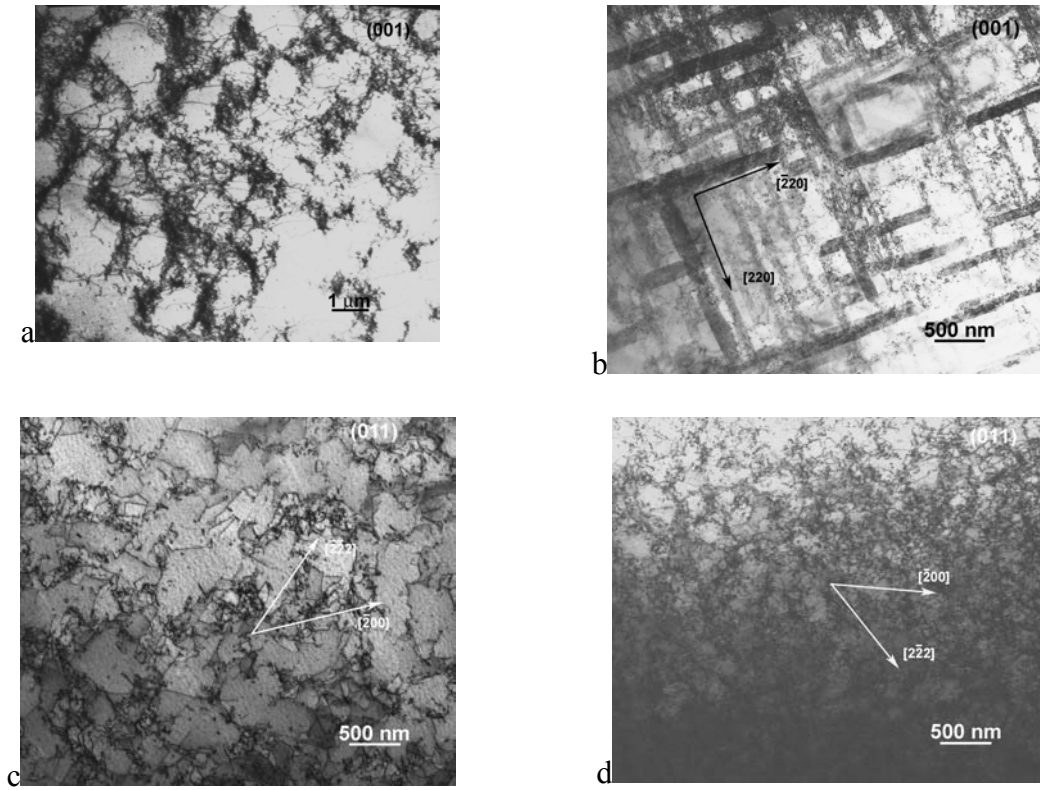

Figure 2. Characteristic defect features for two orientations under the same pressure conditions; (a) & (b): [001] at 20 and 40 GPa; (c) & (d): [134] at 20 and 40 Gpa.

The changes in cell size with distance from the energy deposition energy were measured for the [134] orientation. The cell sizes show an increase with distance, consistent with the decay in pressure amplitude shown in Figure 1. The results are plotted in Fig. 3.
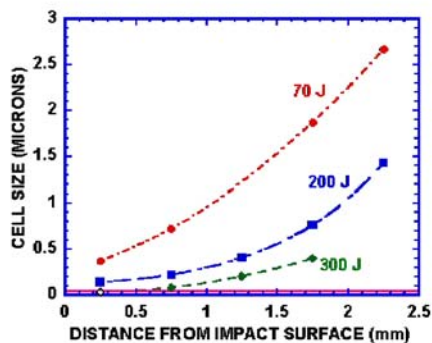

Figure 3. Plot of cell size versus pressure for the three energies

4. ANALYTICAL MODELING

FCC metals have a stacking-fault energy dependent threshold pressures for the initiation of twinning. If one assumes that slip and twinning are competing mechanisms, where plastic deformation by slip has a strain rate and temperature dependence well described by the theory of thermally-activated obstacles, then it is reasonable to assume that slip is highly favored at most conditions. This assumption is corroborated by experimental evidence presented in Section 3. The application of this criterion to the shock front necessitates the knowledge of the strain rate. The strain rate at the shock front has been related to pressure by Swegle and Grady [14],

$$P = k_{SG} \dot{\varepsilon}^{1/4} \tag{2}$$

Two separate aspects have to be considered in the analysis: (a) shock heating, and (b) plastic strain at the shock front. Both shock heating and plastic strain by slip (and the associated work hardening) alter the flow stress of material by slip processes and need to be incorporated into the computation. The shock temperature, T_S, is a thermodynamic function of pressure. It is obtained from the Rankine-Hugoniot equations and the Grüneisen equation of state. The internal energy of the shocked material is converted into heat through the heat capacity and density as

$$T_S = \frac{(V_0 - V)}{2C_v} P + \frac{\exp[(-\gamma_0 / V_0)V]}{2C_v} \int_{V_0}^{V} P \cdot \exp[(\gamma_0 / V_0)V][2 - (\frac{\gamma_0}{V_0})(V_0 - V)]dV \tag{3}$$

Here, V_0 and V are the initial and compressed specific volumes; γ_0 is the Grüneisen parameter for the material; and P and C_v are the pressure and heat capacity, respectively. The total (elastic and plastic) uniaxial strain, ε, at the shock front is related to the change in specific volume by

$$\frac{V}{V_0} = e^{\varepsilon} \tag{4}$$

Inserting Eqn. 4 into the P-V Hugoniot relationship,

$$P = \frac{C_0^2 (1 - e^{\varepsilon})}{V_0 [1 - S(1 - e^{\varepsilon})]^2} \tag{5}$$

The constitutive response of the copper monocrystal is represented by a modified MTS equation

$$\sigma = \sigma_0 f(\varepsilon) \left[1 - \left(\frac{kT}{Gb^3 g_0} Ln \left(\frac{\dot{\varepsilon}_0}{\dot{\varepsilon}} \right) \right)^{2/3} \right]^2 \tag{6}$$

The thermal and strain-rate parameters p, q, g_o, and e_0 are taken from Follansbee and Gray [15]. Values of p=1/2 and q= 3/2, of $g_0 = 0.8$ were used. The work hardening function f(ε) was incorporated by taking a polynomial representation of the stress strain curve for single crystals with the [001] and [$\bar{1}34$] orientations. The [001] orientation is expected to have the lowest threshold pressure for twinning of all orientations, whereas [$\bar{1}34$] should have a substantially higher threshold pressure due to its more gradual hardening. The polynomials used in these calculations are:

[001]: $f(\varepsilon) = 45510\,\varepsilon^6 - 86890\,\varepsilon^5 + 63400\varepsilon^4 - 21830\varepsilon^3 + 2901.8\varepsilon^2 + 464.8\varepsilon^1 - 1.92 \tag{7}$

[$\bar{1}34$]: $f(\varepsilon) = -10871\,\varepsilon^6 + 1431\varepsilon^5 - 7329\varepsilon^4 + 1690\varepsilon^3 + 126.7\varepsilon^2 - 2.344\varepsilon^1 + 0.07 \tag{8}$

For twinning, one just takes a strain rate and temperature independent σ_T. Setting $\sigma_T = \sigma_s$, one can obtain the critical twinning stress as a function of ε, $\dot{\varepsilon}$, and T. Figure 4 shows the predicted threshold for different initial temperatures. It is clear that the [001] orientation has a lower twinning threshold pressure, in agreement with earlier results by De Angelis and Cohen [16].
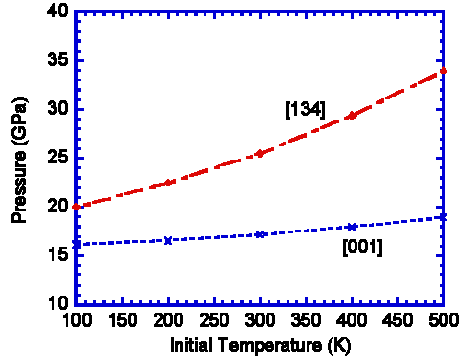
Figure 4. Calculated threshold twinning pressure for [001] and [134] orientation as a function of initial temperature.

5. VOID GENERATION

The feasibility of void nucleation and growth process by a vacancy diffusion mechanism was examined here by taking into account the temperature rise due to shock compression. Cuitiño and Ortiz [17] proposed such a mechanism and its principal characteristics and predictions are given here. This temperature rise is in the range of several hundreds of degrees, depending on the peak shock pressure. The dominating diffusion mechanism is the pipe diffusion along the cores of dislocations (the lattice diffusion being negligible at these temperatures). The diffusion coefficient at the absolute temperature T and for a reference dislocation density is:

$$D(\rho) = \frac{\rho}{\rho_0} D_0 \exp(-Q/kT), \tag{9}$$

where k is the Boltzmann constant, Q is the activation energy of the pipe diffusion mechanism, and D_0 the pre-exponential factor. The reference dislocation density ρ_0 is the dislocation density of an undeformed material. Since the passage of the shock dramatically increases the dislocation density, it significantly enhances the pipe diffusion process. The growth rate is expressed as

$$\frac{dR}{dt} = \frac{1}{R} D(c_0 - c_s) \tag{10}$$

Figure 5 shows the predicted void sizes as a function of time for different temperatures. It is easy to see that diffusion-induced growth cannot occur in the time scale of 10 ns, the tensile pulse time in laser.
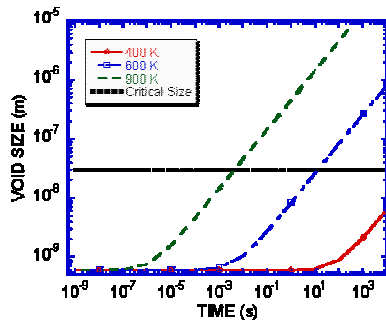

Figure 5. Void size as a function of time for different temperatures for Cuitiño-Ortiz diffusion mechanism.

Therefore, a dislocation-based mechanism was envisaged. The emission of dislocation loops from the surface of the void is postulated as a material transport mechanism. The mechanism is based on the emission of dislocation loops from the surface of the void. Analytical calculations were conducted which show that dislocation emission can occur at a tensile stress of 5 GPa. This is the stress generated by the reflected shock wave at a laser energy of 300 J. Figure 6 shows two types of

loops: prismatic and shear. The concept of dislocation loops to accommodate gradients in plastic strains was introduced by Ashby [18]. This concept is applied to growing voids; the loops generate the geometrically necessary dislocations required to accommodate the plastic strain gradients (Fig. 6c,d).
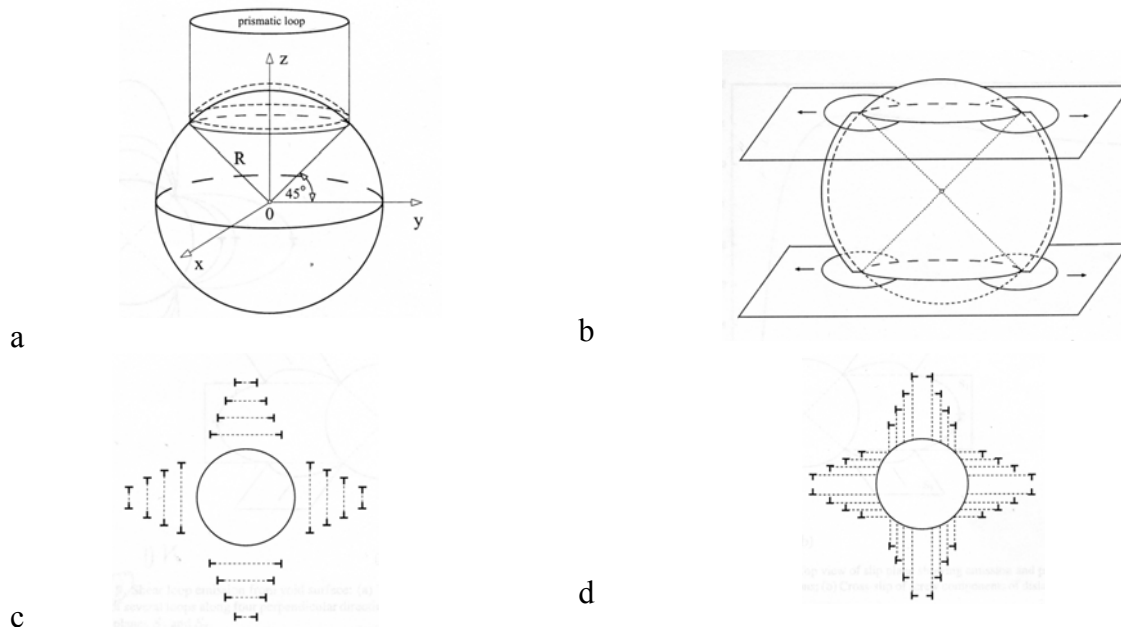

a

b

c

d

Figure 6. Proposed void growth mechanism by dislocation loop emission; (a) prismatic loop emission; (b) shear loop emission; (c) successive prismatic loops; (d) successive shear loops.

REFERENCES

[1] Smith, C.S., *Trans. AIME* **212** (1958) 574.
[2] Johnson, Q., Mitchell, A., Keeler, R.N., and Evans, L., *Phys. Rev. Let*. **25** (1970) 109.
[3] Wark, J.S.,et al. *Phys. Rev. B* **40** (1989) 5705.
[4] Meyers, M.A., Gregori, F., Kad, B.K., Schneider, M.S., Kalantar, D.H., Remington, BA., Ravichandran, G., Boehly, T., *Acta Mat*. **51** (2003) 1211.
[5] Johari, O. and Thomas, G., *Acta Met*. **12** (1964) 1153.
[6] Murr, L.E., in *Shock Waves and High-Strain-Rate Phenomena in Metals*, eds. M.A. Meyers and L.E. Murr, Plenum, NY, 1981, p. 607.
[7] Grace, F.I., *J. Appl. Phys*. **40** (1969) 2649.
[8] Gray III, G.T., in *Shock-Wave and High-Strain-Rate Phenomena in Materials*, eds. M.A. Meyers, L.E.Murr, and K.P. Staudhammer, M. Dekker, NY, 1992, p. 899.
[9]   Hornbogen, E., *Acta Met*. **10** (1962) 978.
[10] Meyers, M.A. *Scripta Met*. **12** (1978) 21.
[11] Weertman, J., in *Shock Waves and High Strain Rate Phenomena in Metals,* Plenum Press. NY, 1981, p. 469.
[12] Mogilevskii, M., Phys. Reports **97** (1983) 359.
[13] Lindl, J., *Phys Plasmas* **2** (1995) 3933.
[14] Swegle, J.W. and Grady, D.E., *J. Appl. Phys*. **58** (1983) 941.
[15] Follansbee, P.S. and Gray III, G.T. *Matls. Sci. and Eng*. **138** (1991) 23.
[16] De Angelis, R.J. and Cohen, J.B., *J. of Metals* **15** (1963) 681.
[17] Cuitiño, A.M. and Ortiz, M., Acta Mat. **44** (1996) 427.
[18] Ashby, M.F., Phil. Mag. **21** (1970) 399.